ELSEVIER

Contents lists available at ScienceDirect

Materials & Design

journal homepage: www.elsevier.com/locate/matdes



Inverse design of 3D cellular materials with physics-guided machine learning



Mohammad Abu-Mualla a, Jida Huang a,*

^a Department of Mechanical and Industrial Engineering, University of Illinois at Chicago, Chicago 60607, IL, United States

HIGHLIGHTS

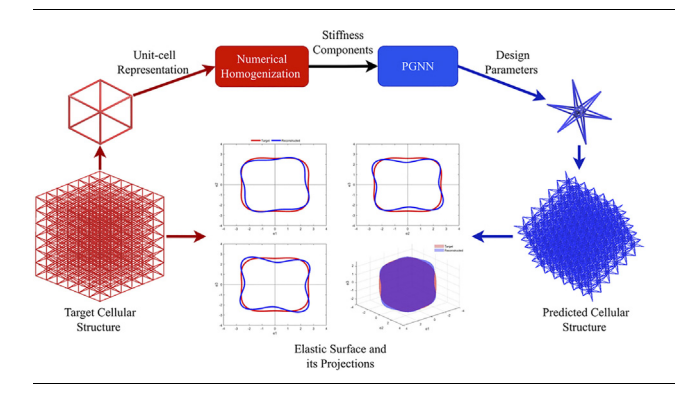
- The PGNN architecture is a promising approach for training a network that can predict design parameters based on design requirements.
- By utilizing a parametrized unit-cells dataset, unit-cells beyond the traditional Cubic or Orthotropic unitcells can be included, providing greater flexibility in the design process.
- Our inverse design framework outperforms search and lookup table methods in terms of accuracy and computational power.

ARTICLE INFO

Article history: Received 22 May 2023 Revised 15 June 2023 Accepted 17 June 2023 Available online 3 July 2023

Keywords: Mechanical metamaterial Cellular structure Inverse design Machine learning

G R A P H I C A L A B S T R A C T



ABSTRACT

This paper investigates the feasibility of data-driven methods in automating the engineering design process, specifically studying inverse design of cellular mechanical metamaterials. Traditional methods of designing cellular materials typically rely on trial and error or iterative optimization, which often leads to limited productivity and high computational costs. While data-driven approaches have been explored for the inverse design of cellular materials, many of these methods lack robustness and fail to consider the manufacturability of the generated structures. This study aims to develop an efficient inverse design methodology that accurately generates mechanical metamaterial while ensuring the manufacturability of predicted structures. To achieve this, we have created a comprehensive dataset that spans a broad range of mechanical properties by applying rotations to cubic structures synthesized from the nine cubic symmetries of cubic materials. We then employ a physics-guided neural network (PGNN) consisting of dual neural networks: a generator network, which serves as the inverse design tool, and a forward network, which acts as a physics-guided simulator. The goal is to generate desired anisotropic stiffness components with unit-cell design parameters. The results of our inverse model are examined with three distinct datasets and demonstrate high computational efficiency and prediction accuracy compared to conventional methods.

© 2023 The Authors. Published by Elsevier Ltd. This is an open access article under the CC BY-NC-ND license (http://creativecommons.org/licenses/by-nc-nd/4.0/).

1. Introduction

Designing advanced materials with tailored properties is a central challenge in materials science and engineering. One promising

solution to alleviate this challenge is discovering metamaterials, an artificial class of materials purposefully engineered to manifest exotic and often unparalleled properties [1]. The exceptional feature of metamaterials is that they exhibit properties mainly determined by their structures rather than their material constituents [2]. Specifically, their topologies are carefully designed to generate

st Corresponding author.

M. Abu-Mualla and J. Huang

Materials & Design 232 (2023) 112103

effective properties not commonly found in natural materials. These properties encompass but are not limited to negative Poisson's ratio [1,3–6], negative index of refraction [7], high stiffness-to-weight ratio [8–11], and mechanical cloaking structures [12]. When designing topologies, one widely used design strategy is discovering cellular materials. *Cellular materials* are a repeated pattern of carefully designed topologies, known as unit-cells, composed of interconnected struts or beams [1]. However, the complexity of such cellular structures and the grand design space of possible geometrical configurations make it challenging to design cellular materials with target properties.

In general, the cellular materials design process involves design formation to validation, known as forward design. Conventional design formation to discover these cellular metamaterials are often limited by their reliance on intuition and trial-and-error methods. which can be time-consuming and resource-intensive [1]. Once designed, these metamaterials are validated through finite element analysis and numerical homogenization [13-15]. These methods rely on differentiable physics solvers to evaluate gradients for each design option during the optimization process, making them challenging to apply in scenarios where performance is evaluated through non-theoretical means, such as experimentation [15,16]. To alleviate the above issues, another common method is to select a suitable mechanical metamaterial candidate that meets predetermined properties by building a cellular materials database [17]. For instance, a large lookup table including approximately 17,000 unit-cell structures was established in [13]. However, this process can also be computationally demanding to validate every single unit structure in the database. As such, an automated cellular materials design process is demanded, i.e., we can computationally generate a cellular structure with desired properties. This automated design process is known as inverse design [18]. The inverse design has emerged as a potent tool for the efficient and systematic design of intricate metamaterial structures in the recent decade [2,8,18-21].

In most existing works, there are two main approaches to achieving the inverse design of cellular materials: optimizationbased and data-driven-based methods. Optimization-based approaches are usually referred to as topology optimization, which is also known as inverse homogenization methods [21,22]. Although these techniques have been extensively utilized in prior research [23-28], they pose a challenge in 3D lattice inverse design, primarily due to their computationally intensive nature. Additionally, the structures generated by these methods may not be easily manufacturable [18,22,29]. Data-driven approaches eliminate the requirement for computationally demanding microscale homogenization procedures and expedite the process of structural optimization [2,8,18–21,30,31]. In addition, data-driven methods are highly suitable for problems with intricate functionality that are not solvable through analytical means [32,33]. Furthermore, data-driven approaches can be seamlessly integrated with preexisting knowledge of the underlying physical laws or principles [32]. Nonetheless, the effectiveness of these methods depends on various factors such as the amount of available training data, statistical robustness, functional complexity, stability, and interpretability. Different trade-offs exist among these factors, which should be carefully considered [33].

Data-driven approaches have been extensively applied in various aspects of engineering research. These include performance prediction [34–36], optimization design [37,38], inverse design [39–41], and damage detection [42,43]. In the specific context of data-driven inverse design for mechanical metamaterials, neural networks (NNs) are commonly employed to uncover the underlying relationship between the design parameters of mechanical metamaterials and their mechanical properties [44]. Convolutional neural networks (CNNs) [45,46] have shown promise in aiding the

inverse design of mechanical metamaterials by learning the optimal arrangement of mechanical elements to achieve desired mechanical properties. Moreover, CNNs outperform NNs in situations where there are a large number of high-dimensional samples. However, the most commonly used techniques in the inverse design of mechanical metamaterials involve the combination of NNs and convolutional neural networks CNNs within dual deep learning networks, such as Generative Adversarial Networks (GANs) and Variational Autoencoders (VAEs). GANs have demonstrated exceptional capabilities in generating diverse and realistic designs [8,47-50], facilitating exploration within the design space and enabling the creation of intricate metamaterial designs that exhibit desired mechanical properties. On the other hand, VAEs [20,51–53] serve as powerful generative models with the capacity to learn intricate patterns and generate diverse designs. Furthermore. VAEs provide a latent space representation, enabling interpolation and exploration of various design variations. This attribute empowers designers to exert control over the properties of generated designs through manipulation of points within the latent space. In recent years, a trend has emerged, combining machine learning with other methods in the design process. This approaches reduce reliance on data alone. Examples include combining topology optimization methods with data-driven approaches [54,55], genetic algorithms with machine learning networks [40,56-58], and Bayesian optimization with machine learning methods [51] for mechanical metamaterial design. This integration signifies a broader and more holistic approach to metamaterial design.

The integration of machine learning algorithms with other algorithms has witnessed a significant increase, with a notable surge of interest in Physics-guided Neural Networks (PGNNs) in recent years [59]. PGNNs networks have garnered considerable attention due to advancements in computing capabilities, making them more practical to employ. Unlike GANs and VAEs, PGNNs do not solely rely on data to emulate a physical system's response. Instead, these models operate within a hybrid modeling framework, utilizing both data and outputs of physics-based model simulations to make predictions that are more readily interpretable using conventional deep learning techniques. In the realm of metamaterial inverse design, dual neural networks in the form of Physics-guided Neural Networks have shown great promise, yielding highly encouraging results [18,60,61]. Notably, Deep Operator Networks (DeepONets) are gaining popularity in modeling as they can effectively learn the underlying operators or differential equations associated with a physical system. This characteristic allows for more general applicability and eliminates the need for retraining or transfer learning when input parameters change [62]. DeepONets have demonstrated strong performance in generalizing PDE problems, surpassing the capabilities of Physics-informed Neural Networks [63,64] due to their general nature. Although the use of DeepONets in the inverse design of mechanical metamaterials is still in its early stages with less number of publications, their potential in the design field is promising due to their ability to handle parameters in a separate branch network [62]. Thus, DeepONets are recommended for future work in inverse mechanical design.

One of the most significant hurdles in data-driven inverse design problems is accurately representing the data, i.e., the unit structures and their material properties in our case. Common methods employed for metamaterial representation include voxelated format [47,49], graph representation [65,66], and parametric representation [18,55,60]. However, voxel representation proves highly inefficient when dealing with sparse 3D cellular materials. The voxel format has the curse of dimensionality issues, connectivity problems, and shape completion complications due to the sparsity of the generated representation. Additionally, both graph and

parametric representations possess the drawback of difficulty in finding a representation that encompasses a broad spectrum of mechanical properties [14,22,66], with a majority of these works concentrating on cubic and orthotropic unit-cells, disregarding the shear-shear and shear-normal coupling components in the effective stiffness tensor of other possible mechanical metamaterials [18]. Parameterization methods possess numerous attractive features for representing unit structures of cellular materials such as their simplicity in terms of comprehension and result interpretation, as well as their rapidity in acquiring knowledge from data with a reduced need for extensive training dataset [67]. As such, we will introduce a new parametric approach for representing cellular structures that can generate not only cubic and orthotropic structures but also anisotropic structures in this work.

In the realm of metamaterial design, manufacturability poses a significant challenge that requires careful consideration of various constraints and requirements, such as feasibility and physical validity, to ensure the physical realization of the desired mechanical structures [1]. Furthermore, the representation of the synthesized metamaterial with intricate details is important to facilitate the fabrication process. It is crucial to confirm that the training dataset can be manufactured using specific manufacturing processes. Regrettably, manufacturability is neglected in most studies on cellular structure inverse design [30]. In this work, we ensure the manufacturability of the dataset with parametric representation by incorporating geometric constraints during the data generation. By constraining the design space to only include manufacturable designs, we reduce the likelihood of producing structures that cannot be fabricated.

In summary, we propose a data-driven inverse design approach to generate 3D cellular metamaterials that possess targeted mechanical properties in this work. The proposed inverse design framework entails harnessing the robustness of the PGNN approach, which is trained on a collection of manufacturable parametrized data encompassing both cubic and highly anisotropic cellular structures. We demonstrate the potential for inverse design framework to revolutionize the field of metamaterial engineering, paving the way for creating materials with tailored properties for a wide range of applications. To this end, the main contributions of the paper are summarized as follows:

- We have presented a robust framework that effectively facilitates the inverse design of cellular mechanical metamaterials utilizing the PGNN method.

- Our framework guarantees the manufacturability of mechanical metamaterials by training the model on a parameterized dataset consisting of manufacturable unit-cells.
- Our parametrization approach encompasses a wide range of unit-cells, including highly anisotropic ones, achieved by applying rotational transformations to cubic unit-cells.

The rest of the paper, as outlined in Fig. 1, is organized as follows. Section 2 outlines the method used for generating highly parametrized anisotropic unit-cells. The inverse design framework is introduced in Section 3, where the underlying principles are discussed. The performance of the data-driven approach on various datasets, including the training dataset, is detailed in Section 4. Lastly, Section 5 concludes the paper by discussing the contributions, limitations, and potential directions for future research.

2. Data generation

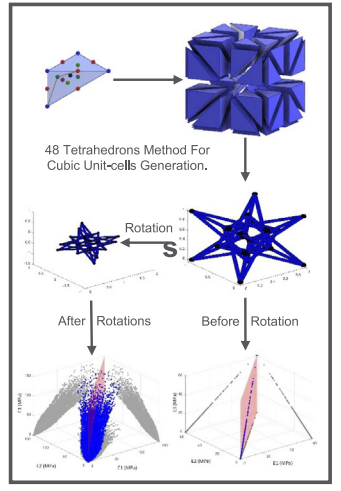
In this section, we present the methodology employed to generate parameterized data required for training our inverse design framework. Specifically, we discuss the numerical homogenization method utilized for computing the mechanical properties of unitcells. Furthermore, we elaborate on the structures generation process, encompassing the application of constraints to ensure the manufacturability of the unit-cells and the approach used for expanding the spectrum of mechanical properties from cubic to more anisotropic behavior.

2.1. Numerical homogenization

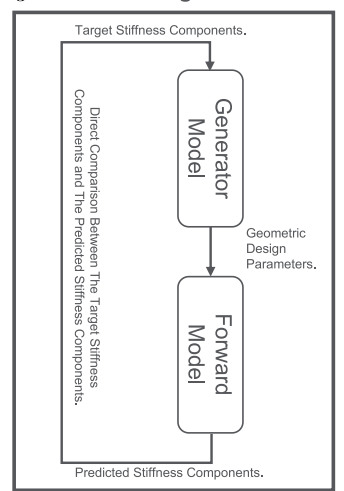
Numerical homogenization is a computational method commonly employed to determine the homogenized macroscopic mechanical properties, or elasticity tensor, of cellular materials [15,68,69]. This technique involves calculating the elasticity tensor using Eq. (1), where E_{ijpq} is the stiffness tensor, v is the virtual displacement field, ϵ_{ij} is the macroscopic displacement in the virtual displacement field, $\epsilon_{pq}^{(olkl)}$ is the prescribed macroscopic displacement, and Ω is the volume of the cellular material, χ^{kl} is the unknown variable we solve for.

$$\int_{\Omega} E_{ijpq} \, \epsilon_{ij}(\nu) \, \epsilon_{pq}(\chi^{kl}) \, d\Omega = \int_{\Omega} E_{ijpq} \, \epsilon_{ij}(\nu) \, \epsilon_{pq}^{0(kl)} \, dV \quad \forall \, \nu \in \Omega$$
 (1)

§2 Data Generation



§3 Inverse Design Framework



§4 Performance Evaluation

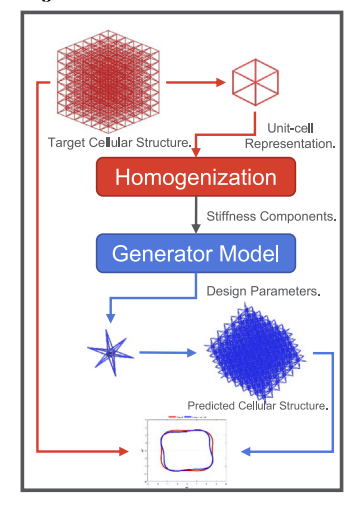


Fig. 1. The overview of the proposed inverse design framework and evaluation.

M. Abu-Mualla and J. Huang

Materials & Design 232 (2023) 112103

The outcome of homogenization analysis is a cellular material's elasticity tensor, which represents its elastic constants. To determine these constants, we conduct six distinct FEA runs, solving Eq. (1) by prescribing three axial and three shear deformations. A detailed description of this method can be found in the reference [15]. The resulting elastic constants are then utilized to calculate the mechanical properties of the cellular material, which form its mechanical profile. It is possible to obtain all the elastic terms using approximation methods such as the Voigt-Reuss-Hill method (VRH) [70], which is based on the elastic stiffness tensor.

2.2. Structure generation

Additive manufacturing has led to the development of numerous unit-cells. However, a significant proportion of these structures pose a challenge in terms of parameterization and exhibit limited material properties. In this study, we address these issues by drawing inspiration from the nine-symmetry planes of cubic materials [14]. Our approach involves creating parametric cubic structures, which are subsequently modified through rotations of the truss structures and their points. This results in a diverse range of properties, which we will demonstrate in the following section. The nine symmetry planes of a cube can divide the cube into identical 48 tetrahedrons, as depicted in Fig. 2(a). Examination of a single tetrahedron reveals 15 distinct nodes, as illustrated in Fig. 2(b). By varying the connections between these nodes and applying reflection along the aforementioned nine symmetric planes, a large number of cubic unit-cell configurations can be generated,

hypothetically amounting to 10³². In this work, we mainly focused on identifying a single unit-cell that can be represented in parametric form and cover a broad spectrum of mechanical properties by adjusting its geometric parameters. To achieve this, we applied certain manufacturability and complexity constraints during the data generation process to limit the number of structures that were explored. The details of our method are presented in the Supplementary material. Ultimately, we selected a unit-cell that is composed of only two edges in each tetrahedron, connecting the v_0, f_3 , and e_2 nodes, as seen in Fig. 3(a). By altering the diameter (1 parameter) and the nodes' offsets (4 parameters) of the chosen unit-cell, we were able to obtain a wide range of cubic behavior. The outcomes of these initial set of parameters generated approximately 4900 unit-cells with a diverse range of bulk mechanical behavior, as shown in Fig. 3(b). The spectrum of properties for various configurations was based on the base material Phrozen Onyx Impact Plus, which has a Young's modulus of 1.175 GPa, Poisson's ratio of 0.35, and a mass density of 1.15 g/cm³.

The unit-cells generated from the methodology depicted in Fig. 3(b) present limitations in diversity and are insufficient to develop a general model, mainly because all of them exhibit cubic symmetry. The anisotropic nature of the stiffness tensor in cellular materials implies that the mechanical properties depend on the orientation of the structure [71]. Therefore we have performed rotations on the cubic unit-cell structure, yielding a broader range of anisotropic configurations. Specifically, we have rotated each of the 4900 unit-cells using an angle θ_{rot} around the rotation axis that was formed by the combination of the unit vectors \mathbf{e}_1 and \mathbf{e}_2 .

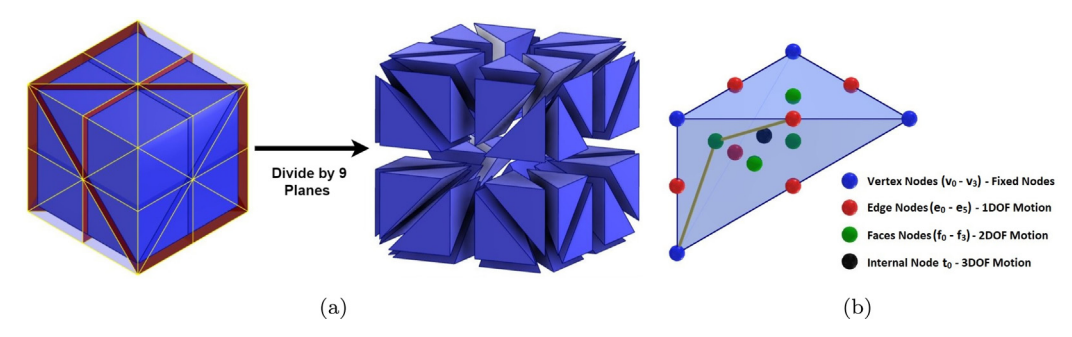


Fig. 2. (a) The tetrahedral cube breakdown is used to generate cellular structures; (b) The node of a single tetrahedron and the motion space of each of the nodes.

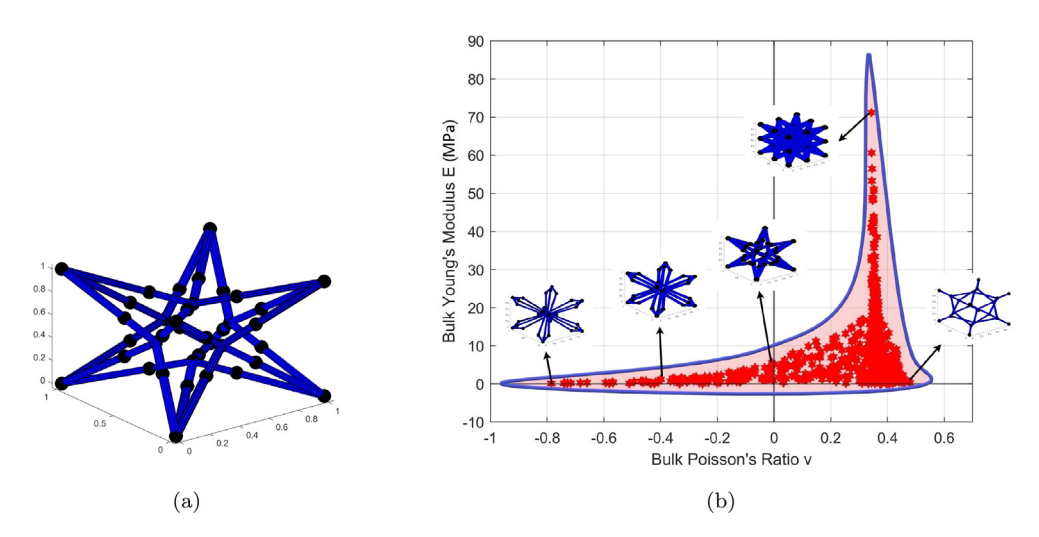
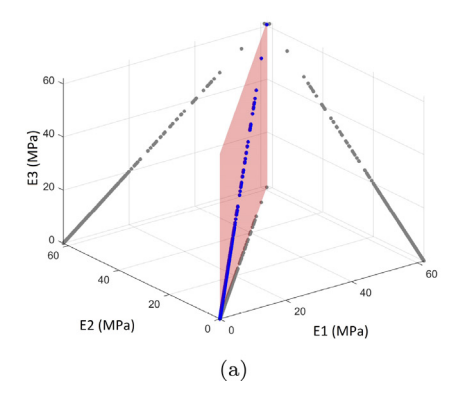


Fig. 3. (a) Basic unit-cell in the proposed parametrization method; (b) Space of Bulk mechanical properties established from the modification of nodes' offsets and truss diameters.



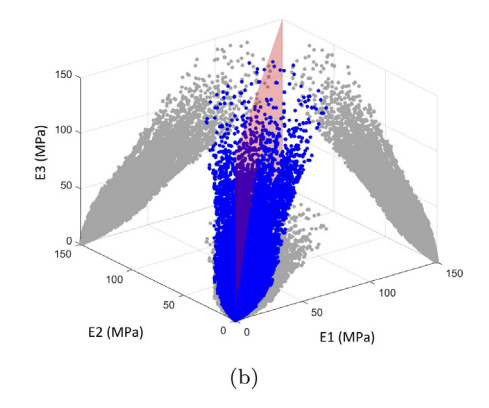


Fig. 4. Effective Young's Modulus space along the unit-cell axes: (a) Cubic configurations without rotations; (b) Cubic configurations after applying rotations.

Nevertheless, utilizing the 3D rotation representation leads to discontinuities in the rotational parameters representation since it repeats every 2π . This discontinuity makes it difficult to train data-driven models that can accurately predict the rotational parameters directly. To address this challenge, we introduced a transformation operation to the initial dataset inspired by [72]. The operation consists of transforming the 3D representation $[\theta_{rot}, e_1, e_2]$ into a 6D representation, and the procedure of rotations is detailed in the Supplementary material. The adoption of the rotation technique enabled the generation of more than 3,000,000 unit-cell configurations. Notably, many of these structures exhibit similar mechanical behavior due to the plane of symmetry of the constituent unit-cell. Moreover, any rotations made along the same coordinate axis with an angle of $k\theta_{rot}$, where kcan be -1 or 1, will produce equivalent configurations and stiffness response. The comparison between the effective Young's modulus range of the dataset before and after the application of rotation is depicted in Fig. 4, and more comparisons of the property space before and after rotation are detailed in the Supplementary material. To this end, we have successfully curated a parameterized training dataset encompassing a diverse range of elastic behaviors.

3. Inverse design framework

The aim of this study is to design a cellular structure that displays desired mechanical behavior. As described in Section 2.1, the elastic properties can be derived from the underlying effective elastic stiffness, which is comprised of 21 distinct components. This section endeavors to establish a trustworthy methodology for generating the 11 geometric variables of the lattice that manifest a prescribed mechanical behavior, which is described by a set of 21 independent elastic parameters. Inverse design is a challenging task because different sets of design parameters can result in similar mechanical properties, and distinct unit-cells can exhibit comparable stiffness responses. This situation is known as an illposed problem. The difficulty arises in determining a measure or loss function that can assess the correctness of a solution while disregarding the existence of multiple valid solutions. Therefore, simply mapping from design parameters to properties, as shown in Eq. (2), using a naive approach can lead to ambiguities when generating cellular structures.

GEN Loss
$$\leftarrow min \frac{1}{n} \sum_{i=1}^{n} \|GEN(C_i) - Par_i\|^2$$
 (2)

To overcome this challenge, we propose an inverse design framework inspired by PGNN models [18,59]. These models incorporate known physics principles and equations into their architecture or training process, combining the strengths of neural

networks and the constraints of physics. In our model, instead of focusing solely on the precise prediction of the design parameters, the objective of our approach is to precisely reconstruct the stiffness tensor of a unit-cell based on a predetermined target stiffness tensor. Our PGNN comprises a generator network (GEN) that predicts unit-cell parameters corresponding to its desired stiffness. This mapping is further constrained using a numerical homogenization simulator (HOM) that determines the stiffness components related to the given unit-cell parameters. In an ideal scenario, we can define a loss function that quantifies the error between the predicted topology's stiffness and the target stiffness, as depicted in Eq. (3). By successfully incorporating this loss function, we transform the inverse problem into a well-posed problem.

INV Loss
$$\leftarrow min \frac{1}{n} \sum_{i=1}^{n} \|HOM(GEN(C_i)) - C_i\|^2$$
 (3)

To enhance efficiency, we exploit the forward network (FOR) introduced in Eq. (4) as a computationally-effective surrogate for the numerical homogenization simulator (HOM). This approach offers a dual advantage. Firstly, the reconstruction loss can be evaluated numerous times using the pre-trained forward network, which is significantly more computationally efficient compared to employing numerical homogenization for reconstruction during PGNN training. Secondly, The introduction of a forward network is crucial as it enables automatic differentiation, a vital aspect of the back-propagation algorithm necessary during the training process. In summary, we have successfully developed an efficient and wellposed PGNN model, as shown in Eq. (5). It is important to note that the forward network is trained independently to improve the accuracy of stiffness value prediction. On the other hand, the generator network is trained within the entire inverse framework, with fixed weights for the forward network, to minimize the error in the generated unit-cell stiffness.

FOR Loss
$$\leftarrow min \frac{1}{n} \sum_{i=1}^{n} \|FOR(Par_i) - C_i\|^2$$
 (4)

INV Loss
$$\leftarrow min \frac{1}{n} \sum_{i=1}^{n} \|FOR(GEN(C_i)) - C_i\|^2$$
 (5)

In Fig. 5, we have presented the specific architecture of the neural networks employed in the training procedure. Given that the values of each parameter can fluctuate across varying ranges, we standardized the parameters in relation to their minimum and maximum values. This normalization procedure guarantees that all parameters are uniformly treated during the training process, with no individual parameter holding greater sway than others. Furthermore, it is recommended to adopt a linear activation

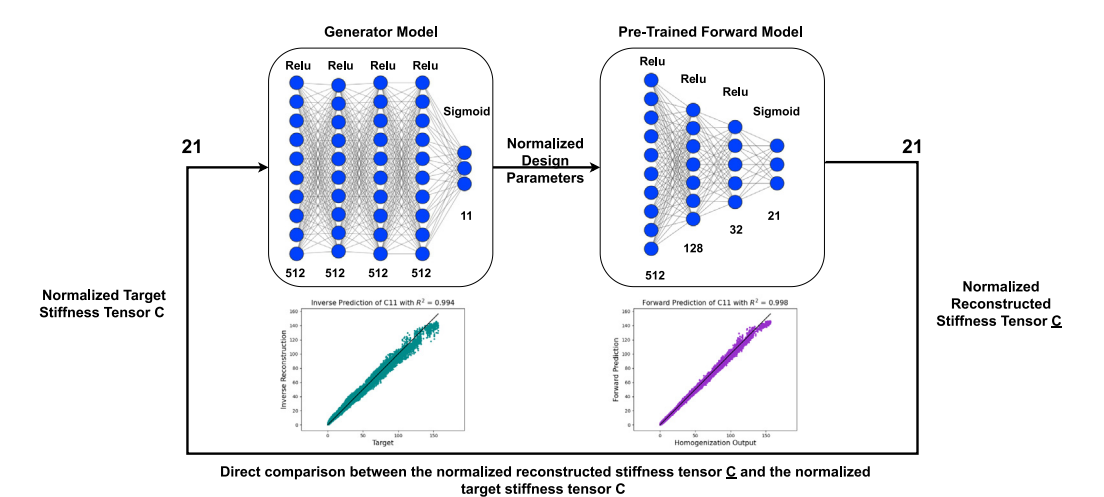


Fig. 5. Inverse Design paradigm based on PGNN consisting of both generator and forward networks.

function, such as ReLU, in the final layer of the architecture for regression problems. Notwithstanding, in our specific architecture, we utilize a Sigmoid activation function in the final layer of both the forward and generator networks, a binary classification activation function. This decision stems from the normalization procedure applied to the data, which guarantees that the output values fall within the range of 0 and 1. Additionally, the application of the Sigmoid function [73] enables the mapping of any input value to a value between 0 and 1. The adoption of the Sigmoid activation function engendered improved outcomes as the model was incapable of being trained utilizing a linear activation function in the last layer. The design of the networks, encompassing the number of layers and the types of activation functions employed in each layer, is exhibited in Fig. 5. Furthermore, we incorporated dropout layers following every hidden layer to forestall overfitting, particularly since there is an imbalance in the data concerning the large values. Our implementation relied on the TensorFlow package¹ that enables automatic differentiation [74], making the implementation of our inverse model effortless. Additionally, we utilized the Adam optimizer [75] to train both the forward and inverse networks, and the mean squared error was employed as the loss function for the two networks.

4. Inverse design performance evaluation

This section aims to assess the efficacy of our proposed inverse design approach. Initially, we examine the prediction results of the training and testing phases with the generated dataset from Section 2. Subsequently, we scrutinize the model's generalizability by testing it on diverse datasets to examine the generalizability of the inverse model. All the experiments in this section are executed on a single Nvidia GeForce RTX 3060 GPU with 16 GB of RAM. The data, source code, and trained models are available in the Supplementary material.

4.1. Network performance with the generated dataset

In our study, we utilized a training dataset of 3,000,000 unitcells, reserving 400,000 for the purpose of testing and validation. The training progress of both the forward and inverse networks is detailed in the Supplementary material. To demonstrate the accuracy of our networks, we have generated correlation plots for the 21 stiffness components of the homogenized stiffness com-

ponent in the forward network, and the correlation between the target and reconstructed stiffness components in the inverse model, for both the testing and training data. Specifically, Fig. 6 presents the correlation plots for C_{11} , while the remaining correlation plots can be referred to in the Supplementary material. Our forward network demonstrates a high degree of precision, as evidenced by the coefficient of determination exceeding 0.984 for all stiffness components. This makes it a viable replacement for the conventional homogenization approach. Similarly, the inverse model is able to reconstruct unit-cells that closely match the target stiffness tensor, with Coefficient of Determination R² values equal to or greater than 0.92 across all stiffness tensor components. Notably, the normal components C_{11} , C_{22} , and C_{33} exhibit particularly high R² values greater than 0.995, whereas the shear-shear coupling components exhibit lower R² values, with the lowest value being approximately 0.92.

A comprehensive evaluation of computational performance is presented in Table 1, encompassing data generation, training, and utilization of our framework. It can be observed from Table 1 that our forward data-driven approach demonstrates notable efficiency in terms of runtime when compared to the conventional homogenization method. Specifically, numerical homogenization utilizing MATLAB necessitates an average of 27.079 seconds for a single structure stiffness calculation, whereas our forward network achieves comparable results with only microseconds of computational power. Similarly, the inverse reconstruction time is likewise in microseconds, further highlighting the high computational efficiency of our model. It is noteworthy that the training time can be further optimized by implementing early stopping for both the forward and inverse model training. After 100 epochs, the loss slightly decreases, as evident from the loss graphs in Supplementary Fig. 6, indicating that further epochs may not be necessary.

4.2. Network performance with other datasets

To extend the evaluation of the effectiveness of our inverse model, we have conducted experiments to reconstruct cellular structures from our model space that exhibit analogous stiffness tensors to those structures from other datasets. This approach is rooted in the premise that dissimilar structures can lead to similar stiffness tensors. We have utilized the Normalized Mean-Squared Error (NMSE) as a quantitative metric, as defined in Eq. (6), to facilitate numerical comparison and assess the precision of the reconstructed structure's stiffness tensor with respect to the target stiffness tensor.

¹ https://www.tensorflow.org/

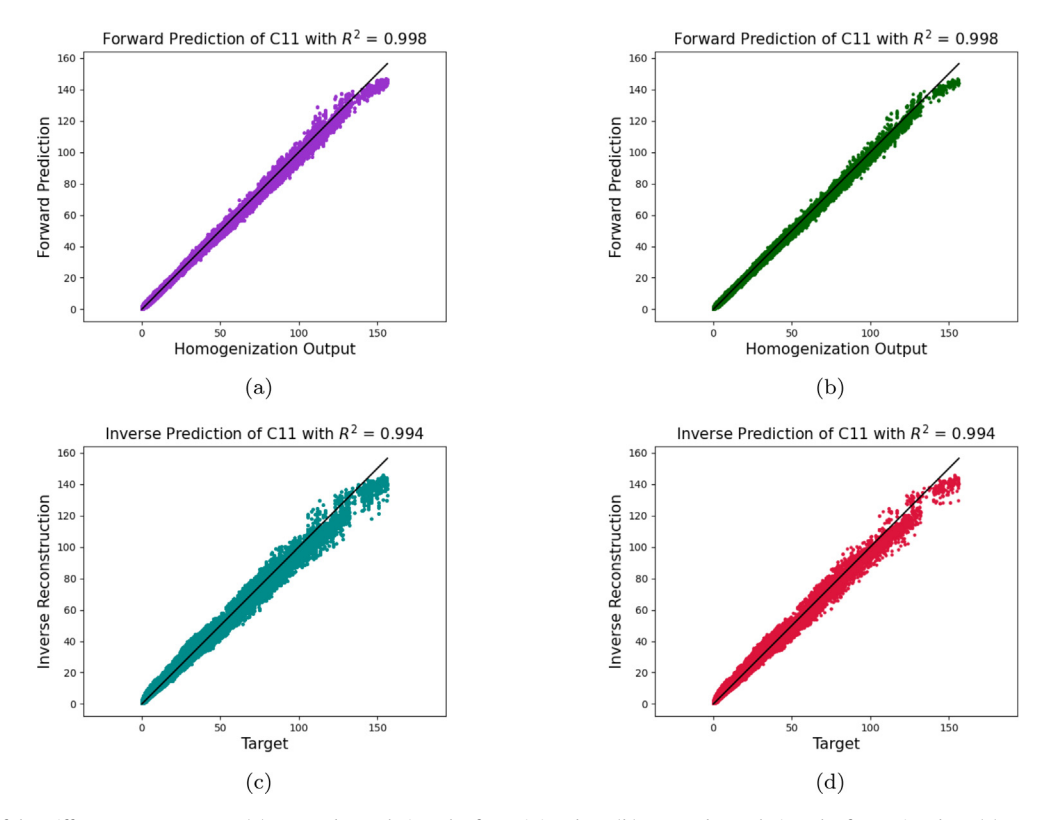


Fig. 6. Comparison of the stiffness component C_{11} : (a) Forward Correlation plot for training data; (b) Forward Correlation plot for testing data; (c) Inverse Correlation plot for training data; and (d) Inverse Correlation plot for testing data.

Table 1Computational run time for each task in the project, and the name of the hardware and the software utilized.

Task	Software	Hardware	Runtime
Homogenization Cubic Structures Generation and Homogenization.	MATLAB 2021b MATLAB 2021b	Single core CPU Single core CPU	27.079 s for one structure 33 h
Unit-cells Rotation	Python	Single GPU	2 min
Forward Network (Training)	TensorFlow + Python	Single GPU	7 min
Forward Network (Prediction)	TensorFlow + Python	Single GPU	0.063 s for 2000 Structures
PGNN Inverse Model (Training)	TensorFlow + Python	Single GPU	34 min 22.5 s
Generator Network (Prediction)	TensorFlow + Python	Single GPU	0.189 s for 2000 Structures

$$NMSE(C_{target}, C_{pred}) = \frac{\sum_{i=1}^{6} \sum_{j=1}^{6} (C_{target, ij} - C_{pred, ij})^{2}}{\sum_{i=1}^{6} \sum_{j=1}^{6} (C_{target, ij})^{2}}$$
(6)

We commence our testing process by subjecting our inverse model to scrutiny using an external dataset that utilizes the cubic tetrahedral method but with varying tetrahedron nodes [v_1 , f_3 , e_4]. The systematic variation of the truss radius within the range of 0.02 to 0.05 resulted in the creation of approximately 4900 distinct configurations, which showcase a diverse range of cubic mechanical behavior as depicted in Fig. 7.

Next, our inverse model was employed to reconstruct truss configurations that are comparable to the newly developed dataset. The frequency distribution of the reconstructed structures based on their NMSE values is illustrated in Fig. 8(a). Notably, 70.37% of the total data exhibit NMSE values that are lower than 0.05, indicating the effective performance of the inverse model. Furthermore, as illustrated in Fig. 8(b), we have compared our new cubic structures with the training dataset to seek configurations

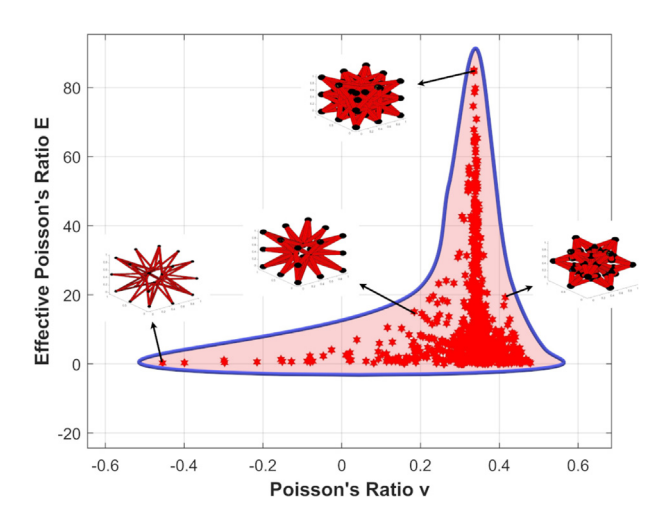
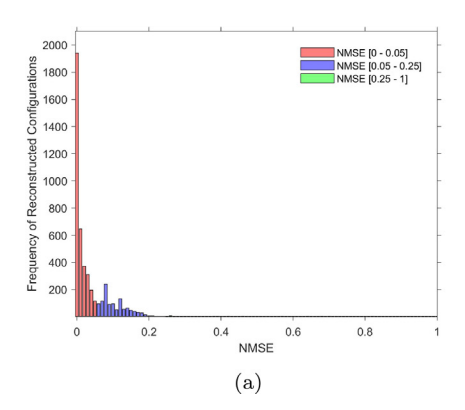


Fig. 7. Space of Properties of unit-cell configurations constructed from $[\nu_1,f_3,e_4]$ tetrahedron nodes.



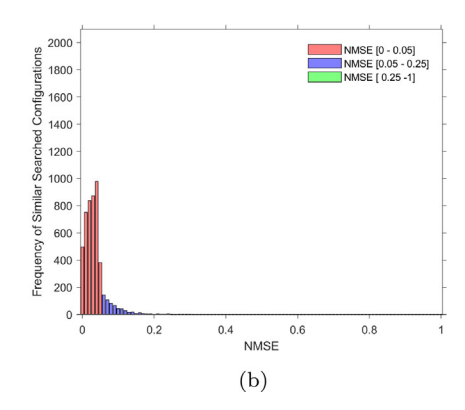


Fig. 8. (a) Histogram of the NMSEs of the inversely reconstructed unit-cells based on the stiffness tensor of Cubic data generated from 48 tetrahedron method with $[v_1, f_3, e_4]$ nodes; and (b) Histogram of the NMSEs of the direct search of unit-cells that have lowest NMSE comparing the training dataset with the Cubic data generated from 48 tetrahedron method with $[v_1, f_3, e_4]$ nodes.

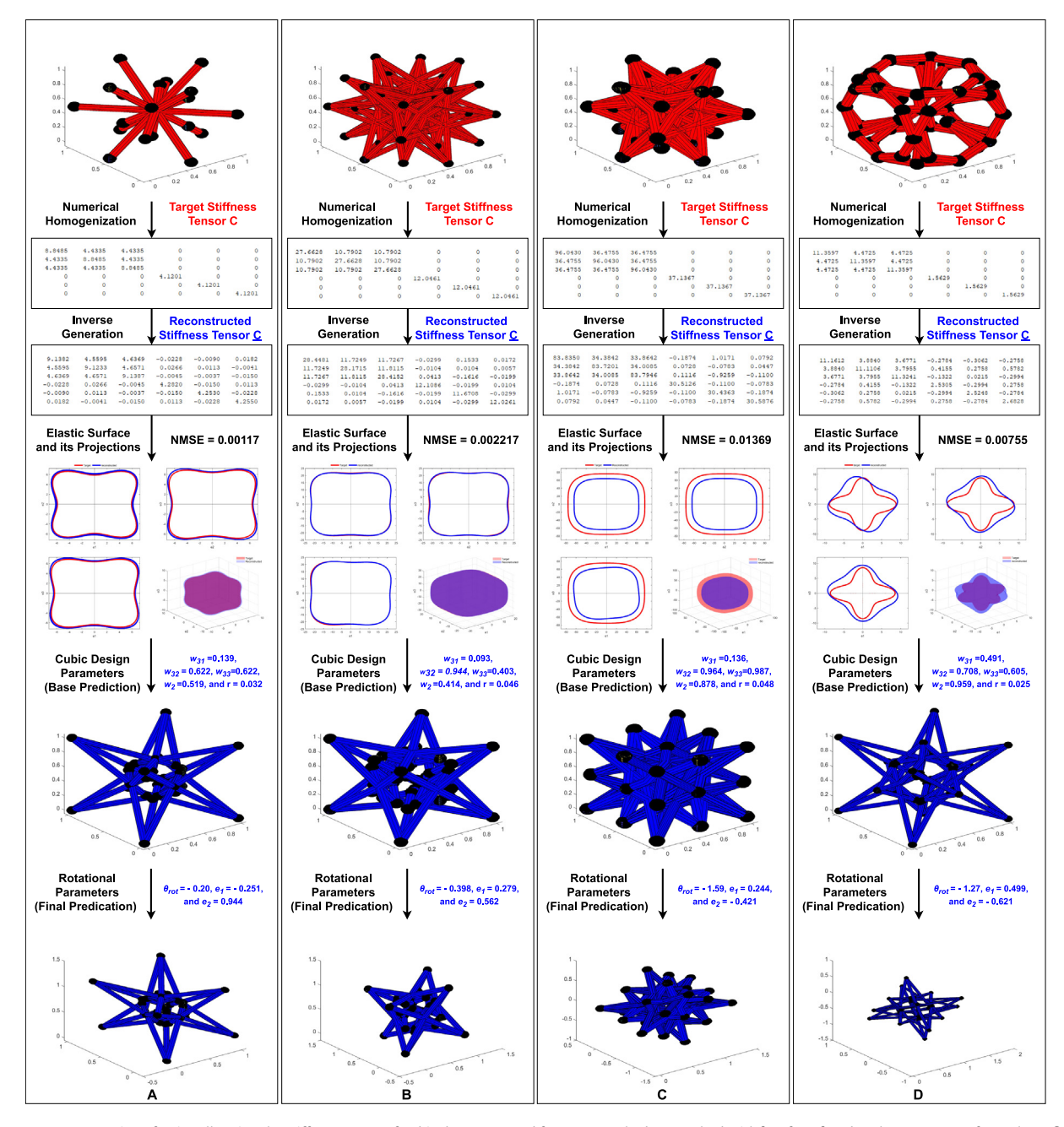


Fig. 9. Inverse reconstruction of unit-cells using the stiffness tensor of Cubic data generated from 48 tetrahedron method with $[v_1, f_3, e_4]$ nodes, the parameters for each configuration: A. w_{31} = 0, w_{32} = 0, w_{33} = 1, w_{4} = 0.6, v_{32} = 0.05, and D. w_{31} = 1, w_{32} = 2/3, w_{33} = 1, w_{4} = 0.2, v_{32} = 1/3, v_{32} = 1/3, v_{32} = 1/3, v_{32} = 1/3, v_{33} = 1, v_{4} = 0.4, v_{32} = 1/3, v_{33} = 1, v_{4} = 0.7, v_{32} = 1/3, v_{33} = 1, v_{4} = 0.7, v_{32} = 1/3, v_{33} = 1, v_{4} = 0.7, v_{32} = 1/3, v_{33} = 1, v_{4} = 0.7, v_{32} = 1/3, v_{33} = 1, v_{4} = 0.7, v_{32} = 1/3, v_{33} = 1, v_{4} = 0.7, v_{32} = 1/3, v_{33} = 1, v_{4} = 0.7, v_{32} = 1/3, v_{33} = 1, v_{4} = 0.7, v_{32} = 1/3, v_{33} = 1, v_{4} = 0.7, v_{32} = 1/3, v_{33} = 1, v_{4} = 0.7, v_{32} = 1/3, v_{33} = 1, v_{4} = 0.7, v_{32} = 1/3, v_{33} = 1, v_{4} = 0.7, v_{32} = 1/3, v_{33} = 1, v_{4} = 0.7, v_{32} = 1/3, v_{33} = 1, v_{4} = 0.7, v_{32} = 1/3, v_{33} = 1, v_{4} = 0.7, v_{32} = 1/3, v_{33} = 1, v_{4} = 1/3, v_{32} = 1/3, v_{33} = 1, v_{4} = 1/3, v_{32} = 1/3, v_{33} = 1, v_{4} = 1/3, v_{32} = 1/3, v_{33} = 1, v_{4} = 1/3, v_{32} = 1/3, v_{33} = 1, v_{4} = 1/3, v_{32} = 1/3, v_{33} = 1, v_{4} = 1/3, v_{32} = 1/3, v_{33} = 1, v_{4} = 1/3, v_{32} = 1/3, v_{33} = 1/3,

Materials & Design 232 (2023) 112103

that display the lowest NMSE. Our findings indicate that the NMSE values of our reconstructed structures surpass the closest match discovered in the training dataset, signifying the superiority of our inverse model over the conventional search or lookup tables method employed in this dataset. Additionally, computing the NMSE values for each configuration's stiffness in the new dataset with every configuration in the three million training dataset consumes over 4,000 minutes for the entire new dataset. Conversely, the inverse design data-driven approach requires only 0.53 seconds to identify the closest stiffness configuration for the entire new testing data, demonstrating the efficiency of our inverse model. Subsequently, we have randomly selected four reconstructed configurations with NMSE values lower than 0.05 and presented them alongside their corresponding original configuration counterparts in Fig. 9, including the comprehensive reconstruction steps. Following that, we assess the model's proficiency by analyzing its performance on the most comprehensive crystallographic trusses dataset obtainable, acquired from Lumpe and Stankovic's [13] scholarly work; a comprehensive description is provided in the Supplementary material. Based on our analysis, it appears that the model's performance in reconstructing structures with stiffness components comparable to the Lumpe and Stankovic dataset is insufficient to establish the generalizability of our approach to all configurations at this time. We observed that only 32% of the reconstructed configurations met the acceptable criteria mentioned earlier, as shown in Supplementary Fig. 11. Therefore, we conclude that the current training dataset is not extensive enough, highlighting the necessity of generating a more diverse and comprehensive parametrize dataset.

The proposed data-driven model offers numerous advantages over existing methods. The inverse design framework is characterized by high efficiency and can predict cellular unit-cells with target stiffness tensors within microseconds, which is orders of magnitude faster than classical computationally-intensive optimization-based methods. In addition, the proposed model outperforms recent data-driven inverse methods, such as those involving iterative search in a latent space [52], which are computationally expensive due to the high dimensionality of predicting the position of hundreds of voxels in metamaterial inverse design [47]. The truss-based model synthesizer ensures manufacturability by utilizing a simple unit-cell base element within its predicted unit-cells, which can be readily fabricated through additive manufacturing processes. This contrasts with previous works where the generated lattices often exhibit complexity [18]. Moreover, the proposed model employs parameterized design, thus eliminating the need for post-processing, a common issue with voxel representations.

5. Conclusions and discussions

Inspired by crystallography, the utilization of cellular structures for designing mechanical metamaterials has emerged as a widely adopted technique in the realm of materials design. Despite notable strides in the development of truss structures, the inverse design of structures possessing targeted stiffness properties continues to present an obstacle. To address this challenge, we have leveraged a physics-guided neural network (PGNN) to forecast truss configurations with tailored anisotropic stiffness. The model incorporates the concept of a dual neural network, consisting of a generator network as the design tool and a forward network that emulates the simulation process within the PGNN while also imposing constraints on the training process. The framework underwent training on an extensive dataset comprising millions of unit-cells. The dataset was generated based on the nine symmetries of cubic materials, with an aim to expand the domain of ani-

sotropic behavior by applying rotational transformations. The resultant dataset encompasses a diverse array of topologies with a wide spectrum of mechanical properties. Subsequently, the proposed model was subject to a rigorous evaluation, comprising several testing dataset. Initially, the model's efficacy was tested on data split from the training dataset, wherein the model demonstrated a performance akin to that observed during training. Then, a cubic dataset was generated, which includes distinct base unitcells and configuration by employing the nine symmetries of the cubic materials approach. The inverse paradigm was then utilized to reconstruct similar unit-cells, wherein a reconstruction accuracy of up to 70% was achieved. During the final stage of the evaluation, we examined the reconstruction of analogous configurations using a broad dataset obtained from Lumpe and Stankovic. However, the lower reconstruction accuracy observed in this phase indicated that the training design space lacked comprehensiveness. The model effectively reconstructed unit-cells possessing mechanical properties similar to those present in the original dataset in microseconds. In summary, the proposed paradigm exhibits formidable capabilities provided that the training data encompasses a broad gamut of mechanical properties.

The present study has offered valuable insights into the implementation of PGNN as a design tool. Future works are anticipated in the following aspects:

- Despite expanding the cubic dataset to encompass a wider range of data by implementing rotations, the base cellular topologies remain restricted. Supplementary Fig. 11 illustrates the model's incapacity to fit all cellular topologies. An intriguing approach is to draw inspiration from tetragonal materials instead of the 48 tetrahedron method; the first possesses the capability to act as the basis for both cubic and tetragonal structures even before applying the rotational transformation.
- The utilization of regression models for training purposes imposes constraints upon the prediction space of structures, thus limiting the range of available design options. This constraint may lead to the prediction of structures that fail to satisfy auxiliary design specifications. The integration of probabilistic layers could be a possible solution, as this can facilitate the creation of multiple topologies to generate prescribed stiffness tensors.
- The methodology used for parameterizing data imposes limitations on the model's ability to generate novel configurations or structures beyond the unit cells used during the training phase, as observed in the Lumpe and Stankovic dataset. Consequently, we suggest exploring alternative structure representations, such as voxel-representation, and try to address the challenges associated with this type of representation.

Data availability

The supplementary material supporting research findings and all the cellular structure data, code, and trained neural networks are available at: https://github.com/DreamLabUIC/Inverse_3D_Truss

Data availability

I have shared my code and data in the paper

Declaration of Competing Interest

The authors declare the following financial interests/personal relationships which may be considered as potential competing

interests: Jida Huang reports financial support was provided by National Science Foundation.

Acknowledgements

We acknowledge the support from the National Science Foundation (NSF) through CDS&E-2245298.

Appendix A. Supplementary data

Supplementary data associated with this article can be found, in the online version, at https://doi.org/10.1016/j.matdes.2023.112103.

References

- [1] X. Yu, J. Zhou, H. Liang, Z. Jiang, L. Wu, Mechanical metamaterials associated with stiffness, rigidity and compressibility: A brief review, Prog. Mater Sci. 94 (2018) 114–173.
- [2] G. Oliveri, J.T. Overvelde, Inverse design of mechanical metamaterials that undergo buckling, Adv. Funct. Mater. 30 (12) (2020) 1909033.
- [3] R.S. Lakes, Negative-poisson's-ratio materials: auxetic solids, Annu. Rev. Mater. Res. 47 (2017) 63–81.
- [4] Z. Wang, C. Luan, G. Liao, J. Liu, X. Yao, J. Fu, Progress in auxetic mechanical metamaterials: structures, characteristics, manufacturing methods, and applications, Adv. Eng. Mater. 22 (10) (2020) 2000312.
- [5] P.U. Kelkar, H.S. Kim, K.-H. Cho, J.Y. Kwak, C.-Y. Kang, H.-C. Song, Cellular auxetic structures for mechanical metamaterials: A review, Sensors 20 (11) (2020) 3132.
- [6] X. Zheng, T.-T. Chen, X. Guo, S. Samitsu, I. Watanabe, Controllable inverse design of auxetic metamaterials using deep learning, Mater. Des. 211 (2021) 110178.
- [7] D.R. Smith, J.B. Pendry, M.C. Wiltshire, Metamaterials and negative refractive index, Science 305 (5685) (2004) 788–792.
- [8] A. Challapalli, D. Patel, G. Li, Inverse machine learning framework for optimizing lightweight metamaterials, Mater. Des. 208 (2021) 109937.
- [9] L.R. Meza, A.J. Zelhofer, N. Clarke, A.J. Mateos, D.M. Kochmann, J.R. Greer, Resilient 3d hierarchical architected metamaterials, Proc. Natl. Acad. Sci. 112 (37) (2015) 11502–11507.
- [10] T. Tancogne-Dejean, M. Diamantopoulou, M.B. Gorji, C. Bonatti, D. Mohr, 3d plate-lattices: an emerging class of low-density metamaterial exhibiting optimal isotropic stiffness, Adv. Mater. 30 (45) (2018) 1803334.
- [11] D.W. Abueidda, R.K.A. Al-Rub, A.S. Dalaq, D.-W. Lee, K.A. Khan, I. Jasiuk, Effective conductivities and elastic moduli of novel foams with triply periodic minimal surfaces, Mech. Mater. 95 (2016) 102–115.
- [12] T. Bückmann, M. Thiel, M. Kadic, R. Schittny, M. Wegener, An elasto-mechanical unfeelability cloak made of pentamode metamaterials, Nature Commun. 5 (1) (2014) 4130.
- [13] T.S. Lumpe, T. Stankovic, Exploring the property space of periodic cellular structures based on crystal networks, Proc. Natl. Acad. Sci. 118(7) (2021) e2003504118.
- [14] J. Panetta, Q. Zhou, L. Malomo, N. Pietroni, P. Cignoni, D. Zorin, Elastic textures for additive fabrication, ACM Trans. Graph. (TOG) 34 (4) (2015) 1–12.
- [15] G. Dong, Y. Tang, Y.F. Zhao, A 149 line homogenization code for threedimensional cellular materials written in matlab, J. Eng. Mater. Technol. 141 (1) (2019).
- [16] S. Rastegarzadeh, S. Muthusamy, J. Huang, Mechanical profile of smooth cellular materials, J. Manuf. Sci. Eng. (2022) 1–14.
- [17] C. Schumacher, B. Bickel, J. Rys, S. Marschner, C. Daraio, M. Gross, Microstructures to control elasticity in 3d printing, ACM Trans. Graph. (Tog) 34 (4) (2015) 1–13.
- [18] J.-H. Bastek, S. Kumar, B. Telgen, R.N. Glaesener, D.M. Kochmann, Inverting the structure-property map of truss metamaterials by deep learning, Proc. Natl. Acad. Sci. 119(1) (2022) e2111505119.
- [19] B. Deng, A. Zareei, X. Ding, J.C. Weaver, C.H. Rycroft, K. Bertoldi, Inverse design of mechanical metamaterials with target nonlinear response via a neural accelerated evolution strategy, Adv. Mater. 34 (41) (2022) 2206238.
- [20] H. Pahlavani, K. Tsifoutis-Kazolis, P. Mody, J. Zhou, M.J. Mirzaali, A.A. Zadpoor, Deep learning for size-agnostic inverse design of random-network 3d printed mechanical metamaterials, arXiv preprint arXiv:2212.12047 (2022).
- [21] F. Dos Reis, N. Karathanasopoulos, Inverse metamaterial design combining genetic algorithms with asymptotic homogenization schemes, Int. J. Solids Struct. 250 (2022) 111702.
- [22] O. Sigmund, Tailoring materials with prescribed elastic properties, Mech. Mater. 20 (4) (1995) 351–368.
- [23] S. Xu, J. Shen, S. Zhou, X. Huang, Y.M. Xie, Design of lattice structures with controlled anisotropy, Mater. Des. 93 (2016) 443–447.
- [24] R.M. Latture, M.R. Begley, F.W. Zok, Design and mechanical properties of elastically isotropic trusses, J. Mater. Res. 33 (3) (2018) 249–263.

- [25] J.K. Lüdeker, O. Sigmund, B. Kriegesmann, Inverse homogenization using isogeometric shape optimization, Comput. Methods Appl. Mech. Eng. 368 (2020) 113170.
- [26] R. Yera, N. Rossi, C. Méndez, A.E. Huespe, Topology design of 2d and 3d elastic material microarchitectures with crystal symmetries displaying isotropic properties close to their theoretical limits, Appl. Mater. Today 18 (2020) 100456.
- [27] S. Rastegarzadeh, J. Wang, J. Huang, Neural network-assisted design: A study of multiscale topology optimization with smoothly graded cellular structures, J. Mech. Des. 145 (1) (2023) 011701.
- [28] J. Wang, J. Huang, Functionally graded non-periodic cellular structure design and optimization, J. Comput. Inf. Sci. Eng. 22 (3) (2022).
- [29] S. Rastegarzadeh, J. Wang, J. Huang, Two-scale topology optimization with isotropic and orthotropic microstructures, Designs 6 (5) (2022) 73.
- [30] L. Zheng, S. Kumar, D.M. Kochmann, Data-driven topology optimization of spinodoid metamaterials with seamlessly tunable anisotropy, Comput. Methods Appl. Mech. Eng. 383 (2021) 113894.
- [31] Y.-C. Hsu, C.-H. Yu, M.J. Buehler, Tuning mechanical properties in polycrystalline solids using a deep generative framework, Adv. Eng. Mater. 23 (4) (2021) 2001339.
- [32] Z. Li, R. Pestourie, Z. Lin, S.G. Johnson, F. Capasso, Empowering metasurfaces with inverse design: principles and applications, ACS Photonics 9 (7) (2022) 2178–2192.
- [33] S. Arridge, P. Maass, O. Öktem, C.-B. Schönlieb, Solving inverse problems using data-driven models, Acta Numerica 28 (2019) 1–174.
- [34] W. Wang, P. Wei, H. Liu, C. Zhu, G. Deng, H. Liu, A micromechanics-based machine learning model for evaluating the microstructure-dependent rolling contact fatigue performance of a martensitic steel, Int. J. Mech. Sci. 237 (2023) 107784
- [35] E. Hu, I.P. Seetoh, C.Q. Lai, Machine learning assisted investigation of defect influence on the mechanical properties of additively manufactured architected materials, Int. J. Mech. Sci. 221 (2022) 107190.
- [36] X. Sun, Z. Liu, X. Wang, X. Chen, Determination of ductile fracture properties of 16mnd5 steels under varying constraint levels using machine learning methods, Int. J. Mech. Sci. 224 (2022) 107331.
- [37] A. Singh, Z. Gu, X. Hou, Y. Liu, D.J. Hughes, Design optimisation of braided composite beams for lightweight rail structures using machine learning methods, Compos. Struct. 282 (2022) 115107.
- [38] C. Kim, J. Lee, J. Yoo, Machine learning-combined topology optimization for functionary graded composite structure design, Comput. Methods Appl. Mech. Eng. 387 (2021) 114158.
- [39] Q. Zeng, Z. Zhao, H. Lei, P. Wang, A deep learning approach for inverse design of gradient mechanical metamaterials, Int. J. Mech. Sci. 240 (2023) 107920.
- [40] Y. Wang, Q. Zeng, J. Wang, Y. Li, D. Fang, Inverse design of shell-based mechanical metamaterial with customized loading curves based on machine learning and genetic algorithm, Comput. Methods Appl. Mech. Eng. 401 (2022) 115571.
- [41] J. Fang, M. Xie, X. He, J. Zhang, J. Hu, Y. Chen, Y. Yang, Q. Jin, Machine learning accelerates the materials discovery, Mater. Today Commun. (2022) 104900.
- [42] Y. Wang, Q. Luo, H. Xie, Q. Li, G. Sun, Digital image correlation (dic) based damage detection for cfrp laminates by using machine learning based image semantic segmentation, Int. J. Mech. Sci. 230 (2022) 107529.
- [43] S. Yoon, W.J. Cantwell, C.Y. Yeun, C.-S. Cho, Y.-J. Byon, T.-Y. Kim, et al., Defect detection in composites by deep learning using solitary waves, Int. J. Mech. Sci. 239 (2023) 107882.
- [44] H. Deng, A.C. To, Topology optimization based on deep representation learning (drl) for compliance and stress-constrained design, Comput. Mech. 66 (2) (2020) 449–469.
- [45] H. Ronellenfitsch, N. Stoop, J. Yu, A. Forrow, J. Dunkel, Inverse design of discrete mechanical metamaterials, Phys. Rev. Mater. 3 (9) (2019) 095201.
 [46] A. Lininger, M. Hinczewski, G. Strangi, General inverse design of thin-film
- [46] A. Lininger, M. Hinczewski, G. Strangi, General inverse design of thin-film metamaterials with convolutional neural networks, arXiv preprint arXiv:2104.01952 (2021).
- [47] X. Zheng, T.-T. Chen, X. Jiang, M. Naito, I. Watanabe, Deep learning-based inverse design of three-dimensional architected cellular materials with the target porosity and stiffness using voxelized voronoi lattices, Sci. Technol. Adv. Mater. (just-accepted) (2022).
- [48] W. Jiang, Y. Zhu, G. Yin, H. Lu, L. Xie, M. Yin, Dispersion relation prediction and structure inverse design of elastic metamaterials via deep learning, Mater. Today Phys. 22 (2022) 100616.
- [49] Y. Mao, Q. He, X. Zhao, Designing complex architectured materials with generative adversarial networks, Sci. Adv. 6 (17) (2020) eaaz4169.
- [50] J. Tian, K. Tang, X. Chen, X. Wang, Machine learning-based prediction and inverse design of 2d metamaterial structures with tunable deformationdependent poisson's ratio, Nanoscale 14 (35) (2022) 12677–12691.
- [51] T. Xue, T.J. Wallin, Y. Menguc, S. Adriaenssens, M. Chiaramonte, Machine learning generative models for automatic design of multi-material 3d printed composite solids, Extr. Mech. Lett. 41 (2020) 100992.
- [52] L. Wang, Y.-C. Chan, F. Ahmed, Z. Liu, P. Zhu, W. Chen, Deep generative modeling for mechanistic-based learning and design of metamaterial systems, Comput. Methods Appl. Mech. Eng. 372 (2020) 113377.
- [53] H.T. Kollmann, D.W. Abueidda, S. Koric, E. Guleryuz, N.A. Sobh, Deep learning for topology optimization of 2d metamaterials, Mater. Des. 196 (2020) 109098.

- [54] S. Rastegarzadeh, J. Wang, J. Huang, Multi-scale topology optimization with neural network-assisted optimizer, International Design Engineering Technical Conferences and Computers and Information in Engineering Conference, Vol. 86212, American Society of Mechanical Engineers, 2022. p. V002T02A041..
- [55] J. Wang, W.W. Chen, D. Da, M. Fuge, R. Rai, Ih-gan: A conditional generative model for implicit surface-based inverse design of cellular structures, Comput. Methods Appl. Mech. Eng. 396 (2022) 115060.
- [56] L. Wu, L. Liu, Y. Wang, Z. Zhai, H. Zhuang, D. Krishnaraju, Q. Wang, H. Jiang, A machine learning-based method to design modular metamaterials, Extr. Mech. Lett. 36 (2020) 100657.
- [57] A.P. Garland, B.C. White, S.C. Jensen, B.L. Boyce, Pragmatic generative optimization of novel structural lattice metamaterials with machine learning, Mater. Des. 203 (2021) 109632.
- [58] Y. Chang, H. Wang, Q. Dong, Machine learning-based inverse design of auxetic metamaterial with zero poisson's ratio, Mater. Today Commun. 30 (2022) 103186.
- [59] A. Daw, A. Karpatne, W. Watkins, J. Read, V. Kumar, Physics-guided neural networks (pgnn): An application in lake temperature modeling, arXiv preprint arXiv:1710.11431 (2017).
- [60] S. Kumar, S. Tan, L. Zheng, D.M. Kochmann, Inverse-designed spinodoid metamaterials, npj Comput. Mater. 6 (1) (2020) 73.
- [61] S. Van't Sant, P. Thakolkaran, J. Martínez, S. Kumar, Inverse-designed growth-based cellular metamaterials, Mech. Mater. 182 (2023) 104668.
- [62] L. Lu, P. Jin, G. Pang, Z. Zhang, G.E. Karniadakis, Learning nonlinear operators via deeponet based on the universal approximation theorem of operators, Nat. Mach. Intell. 3 (3) (2021) 218–229.
- [63] S. Koric, A. Viswantah, D.W. Abueidda, N.A. Sobh, K. Khan, Deep learning operator network for plastic deformation with variable loads and material properties, Eng. Comput. (2023) 1–13.

- [64] S. Korić, D.W. Abueidda, About applications of deep learning operator networks for design and optimization of advanced materials and processes, B&H Electr. Eng. 16 (s1) (2022) 1–6.
- [65] P.P. Meyer, C. Bonatti, T. Tancogne-Dejean, D. Mohr, Graph-based metamaterials: Deep learning of structure-property relations, Mater. Des. 223 (2022) 111175.
- [66] E. Ross, D. Hambleton, Using graph neural networks to approximate mechanical response on 3d lattice structures, Proceedings of AAG2020-Advances in Architectural Geometry 24 (2021) 466–485.
- [67] S.J. Russell, Artificial intelligence a modern approach, Pearson Education Inc, 2010
- [68] A.L. Kalamkarov, I.V. Andrianov, V.V. Danishevs'kyy, Asymptotic homogenization of composite materials and structures, Appl. Mech. Rev. 62 (3) (2009).
- [69] A. Bensoussan, Asymptotic analysis for periodic structures, vol. 374, American Mathematical Soc, 2011.
- [70] R. Hill, The elastic behaviour of a crystalline aggregate, Proc. Phys. Soc. London, Sect. A 65 (5) (1952) 349.
- [71] W.L. Bond, The mathematics of the physical properties of crystals, Bell Syst. Technical J. 22 (1) (1943) 1–72.
- [72] Y. Zhou, C. Barnes, J. Lu, J. Yang, H. Li, On the continuity of rotation representations in neural networks, in: Proceedings of the IEEE/CVF Conference on Computer Vision and Pattern Recognition, 2019, pp. 5745–5753.
- [73] I. Goodfellow, Y. Bengio, A. Courville, Deep learning, MIT Press, 2016.
- [74] M. Abadi, A. Agarwal, P. Barham, E. Brevdo, Z. Chen, C. Citro, G.S. Corrado, A. Davis, J. Dean, M. Devin, et al., Tensorflow: Large-scale machine learning on heterogeneous distributed systems, arXiv preprint arXiv:1603.04467 (2016).
- [75] D.P. Kingma, J. Ba, Adam: A method for stochastic optimization, arXiv preprint arXiv:1412.6980 (2014).